

In the format provided by the authors and unedited.

# Sponge skeletons as an important sink of silicon in the global oceans

Manuel Maldonado <sup>1\*</sup>, María López-Acosta<sup>1</sup>, Cèlia Sitjà<sup>1</sup>, Marta García-Puig<sup>1</sup>, Cristina Galobart<sup>1</sup>, Gemma Ercilla<sup>2</sup> and Aude Leynaert<sup>3</sup>

---

<sup>1</sup>Center for Advanced Studies of Blanes (CEAB), Spanish National Research Council (CSIC), Girona, Spain. <sup>2</sup>Institute of Marine Sciences (ICM-CSIC), Barcelona, Spain. <sup>3</sup>University of Brest, CNRS, LEMAR, Plouzané, France. \*e-mail: [maldonado@ceab.csic.es](mailto:maldonado@ceab.csic.es)

## SUPPLEMENTARY INFORMATION

### Sponge skeletons as an important silicon sink in the global oceans

Manuel Maldonado<sup>1\*</sup>, María López-Acosta<sup>1</sup>, Cèlia Sitjà<sup>1</sup>, Marta García-Puig<sup>1</sup>, Cristina Galobart<sup>1</sup>, Gemma Ercilla<sup>2</sup>, Aude Leynaert<sup>3</sup>

<sup>1</sup>Center for Advanced Studies of Blanes (CEAB). Spanish National Research Council (CSIC), Acceso Cala St. Francesc 14, Blanes, 17300, Girona, Spain.

<sup>2</sup>Institute of Marine Sciences (ICM-CSIC). Passeig Marítim de la Barceloneta, 37-39, Barcelona 08003, Spain.

<sup>3</sup>University of Brest, CNRS, LEMAR, F-29280, Plouzané, France

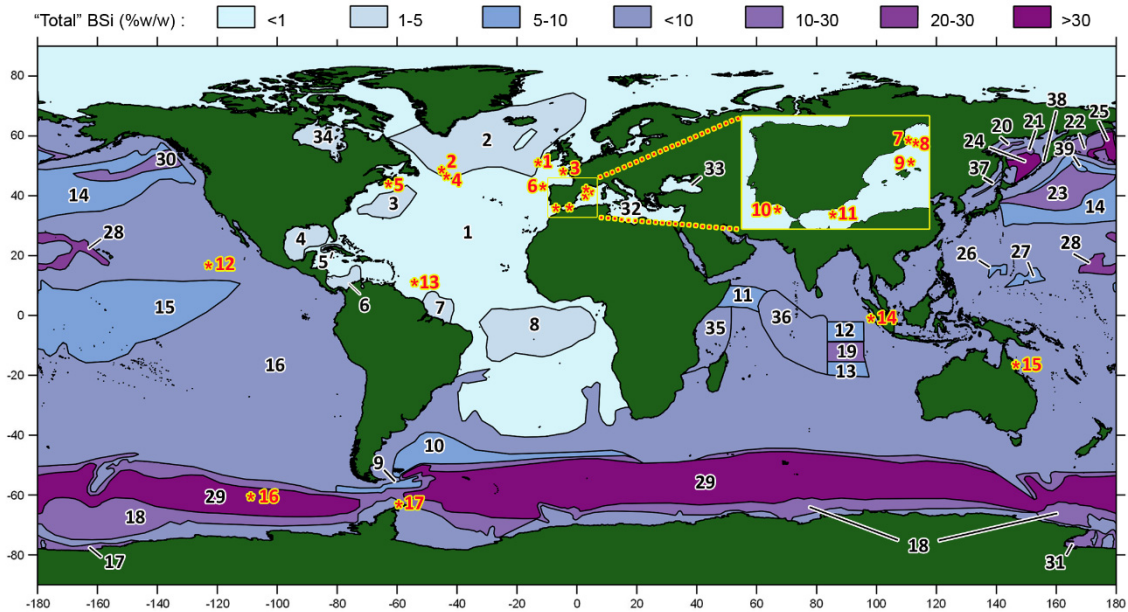
\* Corresponding author: maldonado@ceab.csic.es

**Supplementary Table 1.** Summary of mean ( $\pm$ SD) weight (mg) of siliceous material (W) initially added to be digested in the various digesters, along with the weight (mg) of silicon (Si) contained in each material sample. Eight replicates of each material were digested in each experiment.

MATERIAL		Sodium carbonate			Sodium hidroxide	
		1%	5%	22%	0.2M	0.5M
Frustules of <i>Thalassiosira</i>	W	2.50 $\pm$ 0.00	2.50 $\pm$ 0.00	2.50 $\pm$ 0.00	2.50 $\pm$ 0.01	2.50 $\pm$ 0.01
	Si	1.12 $\pm$ 0.00	1.25 $\pm$ 0.00	1.19 $\pm$ 0.00	1.03 $\pm$ 0.01	1.08 $\pm$ 0.00
Spicules of <i>Petrosia</i>	W	3.00 $\pm$ 0.01	3.00 $\pm$ 0.01	3.00 $\pm$ 0.01	3.00 $\pm$ 0.01	3.00 $\pm$ 0.00
	Si	1.37 $\pm$ 0.00	1.40 $\pm$ 0.00	1.46 $\pm$ 0.00	1.24 $\pm$ 0.00	1.34 $\pm$ 0.00
Spicules of <i>Chondrilla</i>	W	3.33 $\pm$ 0.01	3.33 $\pm$ 0.01	3.33 $\pm$ 0.00	3.33 $\pm$ 0.00	3.33 $\pm$ 0.01
	Si	1.27 $\pm$ 0.00	1.35 $\pm$ 0.00	1.27 $\pm$ 0.00	1.16 $\pm$ 0.00	1.16 $\pm$ 0.00
Bentonite	W	8.98 $\pm$ 0.01	8.99 $\pm$ 0.01	8.98 $\pm$ 0.01	8.98 $\pm$ 0.01	8.98 $\pm$ 0.00
	Si	1.26 $\pm$ 0.00	1.26 $\pm$ 0.00	1.26 $\pm$ 0.00	1.26 $\pm$ 0.00	1.26 $\pm$ 0.00
Kaolinite	W	6.44 $\pm$ 0.01	6.44 $\pm$ 0.01	6.43 $\pm$ 0.01	6.44 $\pm$ 0.01	6.44 $\pm$ 0.01
	Si	1.26 $\pm$ 0.00	1.26 $\pm$ 0.00	1.26 $\pm$ 0.00	1.26 $\pm$ 0.00	1.26 $\pm$ 0.00

**Supplementary Table 2.** Summary of core features, including original cruise labels, geomorphological and geographical settings, coordinates, and depth. Core numbers were given according to North-to-South latitude of the collection site. See [Supplementary Discussion 1](#) for further details and references.

Core #	Core label	Ocean or sea	Seafloor compartment	Geographical site	Latitude (°)	Longitude (°)	Depth (m)
1	51719_13	NE Atlantic	Slope basin	Porcupine Seabight	51.058	-12.912	2025
2	FC062	NW Atlantic	Seamount	Flemish Cap	48.7728	-45.46625	1163
3	KS34	NE Atlantic	Continental shelf	Bay of Brest	48.3133	-4.40945	15.5
4	0058A	NW Atlantic	Seamount	Geodia ground, Flemish cap	46.8487	-43.750446	830
5	MLB2017	NW Atlantic	Continental shelf	Vazella ground, Sambro Bank	43.89	-63.076	160
6	K11	NE Atlantic	Seamount	Galicia Bank	42.8848	-11.56047	2119
7	C2000	Mediterranean	Continental shelf	Portlligat	42.2917	3.29001	3
8	TG36	Mediterranean	Continental rise	Girona	42.017	3.902	1900
9	KF14	Mediterranean	Basin	Balearic Sea	40.527	3.50166	2070
10	TG51bis	NE Atlantic	Continental shelf	Gulf of Cadiz	36.7818	-6.96633	124
11	ALM6	Mediterranean	Basin	Alboran Sea	36.3562	-2.61866	1456
12	JC120	NE Pacific	Abbyssal plain	Equatorial Northeastern Pacific	16.9132	-122.99695	4290
13	TG3	NW Atlantic	Continental rise	Adjacent to Demerara Plain	11.1964	-54.36472	4739
14	SO200	Indian Ocean	Continental slope	Sumatra	-0.8594	97.81493	3840
15	75/GC05	SW Pacific	Continental slope	Great Barrier Reef	-16.42	146.21	1100
16	PC501	SE Pacific	Abbyssal plain	Southern Ocean	-60.5347	-108.3028	5204
17	TG15	SW Atlantic	Continental slope	Antarctic Peninsula	-62.9319	-59.4631	882



**Supplementary Fig. 1 | Geographical location of examined sediment cores relative to the distribution of “total” BSi at the seafloor** (updated after Lisitzin<sup>1,2</sup>, Hurd<sup>3</sup>, and Dittler<sup>4</sup>). Sampled sediments (yellow asterisks and numbers) represent a wide variety of marine environments. Cores were numbered in increasing order according to the latitude of the collection site, from North to South. Further information on cores can be found in [Supplementary Table 1](#) and in [Supplementary Discussion 1](#). Pioneering work by Lisitzin summarized the gross distribution of “total” BSi (as weight % of dry sediment) in the uppermost sediment layer of the world’s oceans. He did it so by digesting 2000 sediment samples in hot 5% sodium carbonate for 5 hours, a method herein demonstrated to dissolve only  $53.76 \pm 1.98\%$  and  $48.81 \pm 2.45\%$  of the spicules mass of *Petrosia ficiformis* and *Chondrilla caribensis*, respectively. Therefore, it underestimated about 50% of the sponge BSi in the sediments. Despite that shortcoming, the gigantic Lisitzin’s work became of widespread importance. It established the notion of 3 “belts” of recent BSi accumulation, grossly reflecting global patterns of abundance of diatoms and radiolarians in the water column: 1) an almost continuous, 1000 to 2000 km-wide band around the globe in the Southern Ocean, with a northern limit at the Antarctic Convergence (45°S to 55°S); 2) an equivalent similar northern band, better developed in the Pacific, Japan Sea and Bering Sea; and 3) a nearly-equatorial 20°N-20°S band in the Indian and Pacific Oceans, which is less marked in the Atlantic Ocean. Lisitzin’s mapping also established the notion that siliceous sediments are poorly represented between the parallels 20° and 40° in northern and southern hemispheres, roughly coincidentally with zones of low abundance of diatoms and radiolarians in the plankton<sup>2</sup>. Those general patterns fostered the view that the BSi accumulating at the ocean bottom proceeded almost exclusively from a rain of siliceous planktonic organisms, which indirectly led to consider as irrelevant any further attempt to estimate the BSi contribution from benthic organisms. Despite the significance of Lisitzin’s work, the truth is that the method he used to digest sediments missed not only about half of the sponge BSi, but, as noticed by DeMaster<sup>5</sup>, it also dissolved an undetermined amount of lithogenic silica, for which no correction was ever applied. Here we have shown ([Fig. 1](#)) that his method dissolves aluminum-silicate bentonite and kaolinite in about  $11.95 \pm 0.34\%$  and  $3.08 \pm 0.12\%$ , respectively.

**Supplementary Discussion 1.** The investigated cores stand for a wide array of depositional environments. Continental shelves are represented by core 3 (Bay of Brest, France, North Eastern Atlantic)<sup>6</sup>, core 5 (Sambro Bank, Canada, North Western Atlantic)<sup>7,8</sup>, core 7 (Portlligat Bay, Spain, Western Mediterranean)<sup>9,10</sup>, and core 10 (Gulf of Cadiz, Spain, North Eastern Atlantic)<sup>11</sup>. All 5 cores account for markedly different depositional environments. For instance, cores 3 and 7 come from shallow bays, but the former with high primary productivity and a detrital bottom hosting a rich sponge community<sup>12</sup>, while the latter has oligotrophic conditions and a sandy bottom almost entirely occupied by a sea grass meadow and a comparatively poor sponge fauna. Yet this

latter bay appears to function as a concentration area that accumulates resuspended materials from adjacent shelf bottoms, what would explain the abundance of sponge spicules, including skeletal pieces from species that are not known to live within the bay. Cores 5 and 10 come from the distal zone of the continental shelf, and, more importantly, core 5 accounts for a dense monospecific aggregation of the hexactinellid sponge *Vazella pourtalesii*<sup>13</sup>, while core 10 comes from a deltaic area with sediments at the distalmost continental shelf, where sponges are rare.

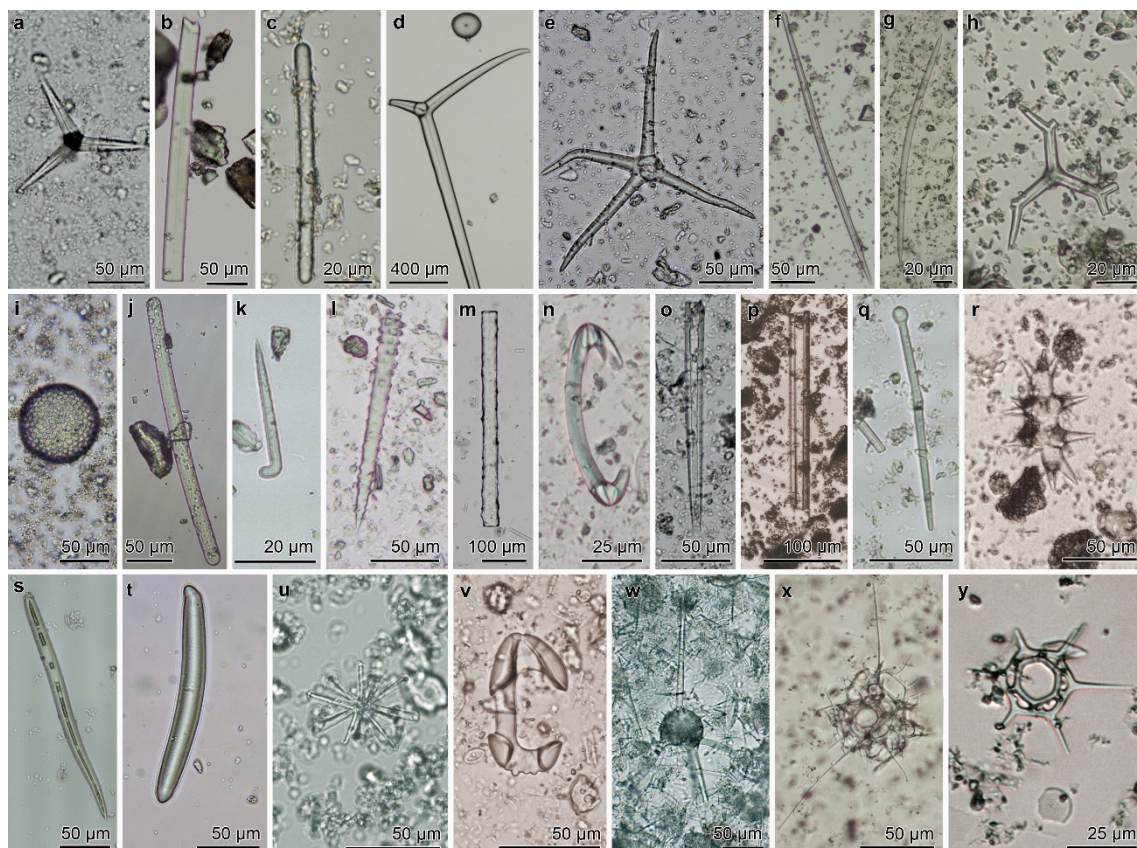
Continental slopes are represented by cores 14 (Sumatra margin, Eastern Indian Ocean), 15 (North Eastern Australian, Great Barrier Reef Slope, Western Pacific), and 17 (Antarctic slope, Southern Ocean). Cores 14 and 15 are from sediments receiving deposition from coral reef assemblages above<sup>14,15</sup>. Core 17 received deposition from rich siliceous benthic and planktonic communities in the area of the Bransfield Strait (Antarctica)<sup>16,17,18</sup>.

Seamounts and plateaus are represented by cores 2, 4, and 6. The latter core receives deposition from the sponge-rich benthic community at the Galicia Bank seamount (Northeastern Atlantic)<sup>19,20,21</sup>. Cores 2 and 4 come from the slope of Flemish Cap Plateau (Northwestern Atlantic, off Canada)<sup>22,23,24</sup>, but core 4 was sampled from an aggregation of *Geodia* spp. sponges, while core 2 is from an area with scarce sponge presence. It is also worth noting the peculiarity of the Recent depositional environment in core 2, with Holocene sedimentation rates (0.01-0.02 mm y<sup>-1</sup>) being sufficiently low and bottom current strength sufficiently high to erode away modern sediments, minimizing rates of BSi accumulation in the upper sediments and burial. The layer of exposed sediment at the bottom, according to correlations with Heinrich Layer stratigraphy<sup>25</sup>, appears to be about 12 ky old, therefore reflecting a combination of Pleistocene preservation and Holocene deposition.

The continental rise is represented by cores 8 and 13. The former receives deposition from productive pelagic communities of the Gulf of Lion (Northwestern Mediterranean), influenced by the terrestrial inputs of seasonal Girona rivers<sup>26</sup> and Rhône River<sup>27,28</sup>. Core 13 (Subequatorial Southwestern Atlantic) receives the depositional influence from the Orinoco River mouth<sup>29,30</sup> and is adjacent to Demerara Abyssal Plain. Because their open-water nature, those sediments were included in the “basin” compartment. Both areas are poor in sponge fauna.

The basin bottoms are represented by cores 1, 9, 11, 12, and 16, but, again, with important between-core differences in depositional environments. Core 1 (Southwest of

Ireland, Northeastern Atlantic)<sup>31</sup>, located in the northern zone of the slope basin “Porcupine Seabight”, might receive depositions from local sponge aggregations<sup>32,33</sup>. Cores 9<sup>34</sup> and 11<sup>35,36</sup> are both receiving deposition from Mediterranean oligotrophic areas and comparatively sponge-poor benthic communities. Yet core 9 (northern Balearic Sea)<sup>37</sup> represents even a less productive Mediterranean zone than core 11 (Alboran Sea)<sup>38</sup>, since the latter might occasionally receive material from benthic assemblages on adjacent banks<sup>39</sup>. Core 12 (Subequatorial Northeastern Pacific)<sup>40</sup> receives deposition from both pelagic communities fostered by rich-nutrient upwellings and abyssal benthic communities from the adjacent Clipperton-Clarion Fracture Zone (CCFZ)<sup>41</sup>, although with scarce sponges. Core 16 (Southern Ocean) receives deposition from rich planktonic communities commonly dominated by siliceous microorganisms and builds a benthic environment that facilitates BSi preservation<sup>42,43,44</sup>, leading to formation of biosiliceous oozes.



**Supplementary Fig. 2 | Sponge, radiolarian and silicoflagellate BSi in sediments.** a-n, Sponge spicules in the superficial sediment of core #1 (a), #2 (b), #3 (c), #4 (d), #5 (e), #8 (f), #9 (g), #11 (h), #12 (i), #13 (j), #14 (k), #15 (l), #16 (m), and #17 (n). o-v, Sponge spicules buried at 50 cm in core #1 (o), #2 (p), #3 (q), #6 (r), #10 (s), #13 (t), #14 (u), and #15 (v). w-x, Radiolarian skeletons in the superficial sediment of core 16 (w) and buried at 50 cm in core 17 (x). (y) Silicoflagellate skeleton buried at 50 cm in core 17. Note that delicate tiny spicules of demosponges (r, v) and hexactinellid (u) sponges are well preserved even after being buried for 14.7, 3.6 and 1.6 kiloyears, respectively.

**Supplementary Table 3.** Contribution (average  $\pm$  SD) of diatoms, sponges, radiolarians and silicoflagellates to the BSi content in the 1-cm thick uppermost layer of sediments.

core #	BSi in uppermost sed. (mg Si g <sup>-1</sup> sed.)			
	diatoms avg $\pm$ SD	sponges avg $\pm$ SD	radiolaria avg $\pm$ SD	silicoflagellates avg $\pm$ SD
1	1.875 $\pm$ 0.436	0.080 $\pm$ 0.034	0.148 $\pm$ 0.005	0 $\pm$ 0
2	2.383 $\pm$ 0.514	1.275 $\pm$ 0.284	0.242 $\pm$ 0.132	0 $\pm$ 0
3	1.472 $\pm$ 0.169	1.391 $\pm$ 0.241	0 $\pm$ 0	0 $\pm$ 0
4	0.142 $\pm$ 0.310	76.314 $\pm$ 38.147	0.078 $\pm$ 0.079	0 $\pm$ 0
5	0.424 $\pm$ 0.165	0.334 $\pm$ 0.026	0.001 $\pm$ 0.000	0.0004 $\pm$ 0.0001
6	0.515 $\pm$ 0.123	2.491 $\pm$ 0.297	0.042 $\pm$ 0.017	0 $\pm$ 0
7	0.022 $\pm$ 0.033	0.496 $\pm$ 0.300	0 $\pm$ 0	0 $\pm$ 0
8	1.073 $\pm$ 0.101	0.012 $\pm$ 0.007	0 $\pm$ 0	0 $\pm$ 0
9	1.033 $\pm$ 0.131	0.045 $\pm$ 0.064	0 $\pm$ 0	0 $\pm$ 0
10	1.029 $\pm$ 0.066	0.042 $\pm$ 0.023	0.0001 $\pm$ 0.0001	0 $\pm$ 0
11	0.701 $\pm$ 0.123	0.061 $\pm$ 0.034	0 $\pm$ 0	0 $\pm$ 0
12	0.715 $\pm$ 0.190	0.135 $\pm$ 0.026	0 $\pm$ 0	0 $\pm$ 0
13	1.228 $\pm$ 0.120	0.287 $\pm$ 0.069	0 $\pm$ 0	0 $\pm$ 0
14	2.471 $\pm$ 0.249	1.044 $\pm$ 0.896	0.051 $\pm$ 0.050	0 $\pm$ 0
15	0.333 $\pm$ 0.166	0.587 $\pm$ 0.042	0.015 $\pm$ 0.018	0 $\pm$ 0
16	98.564 $\pm$ 8.534	0.125 $\pm$ 0.003	5.936 $\pm$ 1.301	0.173 $\pm$ 0.044
17	45.692 $\pm$ 2.316	2.572 $\pm$ 0.861	0.026 $\pm$ 0.010	0 $\pm$ 0

**Supplementary Discussion 2.** The abundance of sponge BSi in sediments, herein quantified for the first time, was long suspected. For instance, several Ocean Drilling Program Reports warned literally that "the scarcity of studies on sponge spicules is not because of a lack of spicules, as spicules are often abundant in marine sediments"<sup>45,46</sup>. Microscopy inspection of sediments from the continental rise and abyssal plane at the Gulf of Mexico ranked spicules as "abundant" to "dominant", whereas diatoms and radiolarians were only "frequent" to "common". Sponge spicules also occurred in 96% of the 1,426 sediment samples collected from open waters deeper than 200 m in the North Atlantic<sup>47</sup>. Spicules have been reported to dominate BSi sediments of coral reefs<sup>48</sup> and rocky coasts<sup>49</sup>. They also form meter-thick mats at the continental shelf and slope in Arctic and Antarctic areas<sup>50,51</sup>.

**Supplementary Discussion 3.** Sponges are sessile organisms. Unlike in the case of diatom frustules, their siliceous spicules do not reach the sediment as a rain from the water column, but experiencing restricted lateral transport and limited resuspension from the decaying sponge bodies. Consequently, rates of deposition and burial of sponge BSi are

little related to the sediment deposition rate ([Supplementary Fig. 5](#)), except for the fact that the faster sediment deposition, the faster the burial of sponge BSi. In general, the magnitude of sponge BSi burial is expected to be more related to both the local abundance of sponge communities<sup>51,52,53,54</sup> and episodic events of massive sponge mortality<sup>55,56</sup>.

Mean rates of sponge BSi burial spanned two orders of magnitude across cores of the “continental-margin-&-seamount” compartment. It reflects the large variety of depositional environments that were sampled. It also means that the approach is considering both the very positive and negative environments in terms of sponge BSi abundance and burial (i.e., sponge aggregations vs. areas with very poor sponge fauna), along with different intermediate situations. In consequence, subsequent additions of information coming from the study of new cores is more likely to reduce the errors associated to our means than to modify substantially the mean themselves. For this reason, our approach is expected to be resilient to the addition of future data.

For calculating preservation of both sponge and radiolarian BSi, a constant rate of BSi deposition within each core for the time period required to build 50 cm of sediment is assumed. Such period ranged from 440 to 14,700 years in the set of cores, being core 12 a 74,000 years-old outlier ([Table 2](#)). There is evidence that some sponge grounds have existed continuously over the last 130 millennia<sup>24</sup>, that glass-sponge reefs have been growing continuously through the last 9,000 years<sup>57</sup>, and that the growth of some giant hexactinellid spicules required up to 11,000 years to be completed<sup>58</sup>. These examples of extreme individual and population longevity indicate that the sponge assemblages, particularly in deep waters, have relatively slow dynamics and that can be stable over periods of millennia. Relatively constant rates of BSi deposition are therefore plausible over the concerned periods.

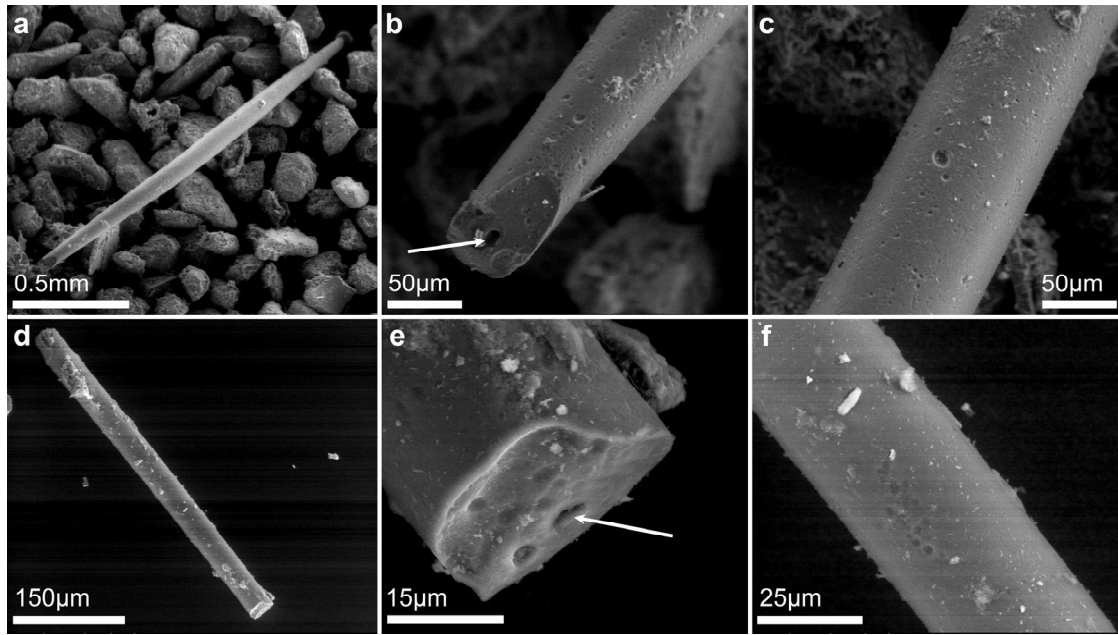
Our approach yielded overrated (>100%) sponge BSi preservation in four cores (i.e., 23.5% of cores). Interestingly, three of those cores (#3, 16, 17) came from sites where rates of accumulation and preservation for diatom BSi are known to be greater than in the rest of the ocean<sup>44,59</sup>. These overrated preservations likely reflect favorable conditions for BSi preservation<sup>44,60,61</sup> coupled to past local episodes of massive mortality in the sponge assemblages<sup>55</sup>. In a fourth core (#8), sponge BSi occurred in extremely low values, the lowest in the study. Under such BSi scarcity, the finding by pure chance of one more or one less spicule in sediment replicates from 0 cm or in those from 50 cm may have an impact on the estimated average preservation (%). For these reasons, overrated cores were never considered when calculating average preservation for sponge BSi. For

subsequent calculations involving the overrated cores, the average BSi preservation ( $45.2 \pm 27.4\%$ ) resulting from the 13 remaining cores was used. This made a conservative approach, since an averaged preservation is used for sediments in which preservation is known to be greater<sup>44,59,62</sup> than the average in marine sediments. Interestingly, the resulting average for sponge BSi preservation comes into general agreement with an approximate 50% decrease in the number of sponge spicules between 0 and 50 cm noticed in the only available studies of coastal sediments in this regard<sup>49,63</sup>.

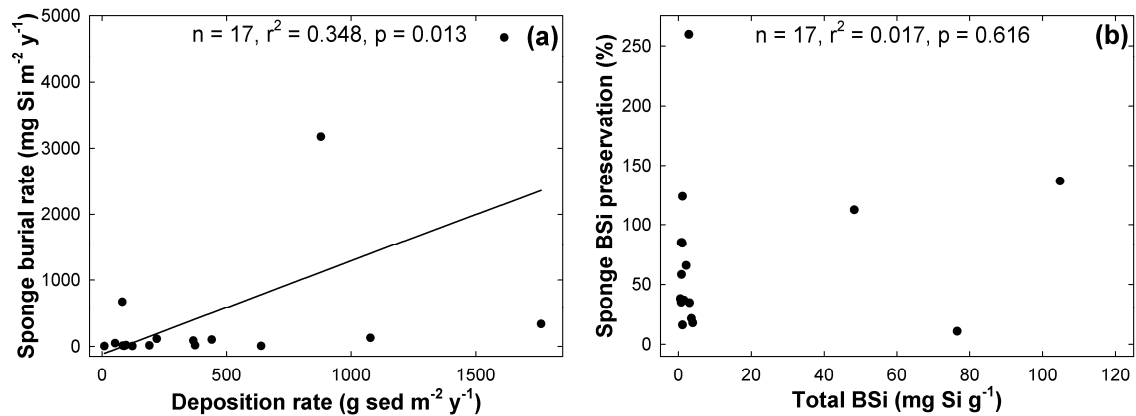
In the case of radiolarians, preservation was also overrated in the same two cores of the Southern Ocean (#16, 17) than sponge BSi did, and, again, in core 10, where radiolarians recorded their lowest abundance. As for sponges, the three overrated cores were never considered when calculating average preservation of radiolarian BSi. Any calculation involving the overrated cores was based on the average preservation value (6.8%) resulting from the rest of cores. In this regard, a scenario considering a radiolarian BSi preservation of only 6.8% in the biosiliceous oozes (scenario 1 in [Supplementary Table 4](#)) can be defined as very conservative. Therefore, we explored two plausible alternative scenarios to evaluate the effect of such constraint. An alternative scenario (scenario 2) was to assume that the preservation of radiolarian BSi in the biosiliceous oozes would be similar to the average preservation (10.2%) estimated for BSi in sediments of the Southern Ocean<sup>62</sup>. Under this scenario, a global burial flux of  $11.3 \pm 5.0 \times 10^{-2}$  Tmol Si  $y^{-1}$  resulted for radiolarians. A third scenario (scenario 3) was to assume a radiolarian preservation in the oozes equal to the maximum preservation found in our set of cores (28.7%). It yielded a global burial flux of  $20.4 \pm 5.6 \times 10^{-2}$  Tmol Si  $y^{-1}$ . Altogether, it means that, even when using relaxed scenarios for BSi preservation, the global burial flux of Si through radiolarian skeletons consistently results in a modest contribution, ranging from 0.09 to 0.20 Tmol Si  $y^{-1}$  ([Supplementary Table 4](#)). The mean point of that interval (0.15 Tmol Si  $y^{-1}$ ) would still represent only 2.4% of the global biological sink.

**Supplementary Table 4.** Mean ( $\pm$ SD) preservation rates and burial fluxes of radiolarian BSi under 3 different scenarios of preservation (%) in the biosiliceous oozes. Scenario 1 assumes preservation of 6.8%, as resulting from the average of the investigated cores, Scenario 3 assumes the maximum preservation found in our set of cores (28.7%). Scenario 2 considers an intermediate preservation (10.7%), which corresponds to the value estimated in the literature<sup>62</sup> for BSi preservation in the Southern Ocean.

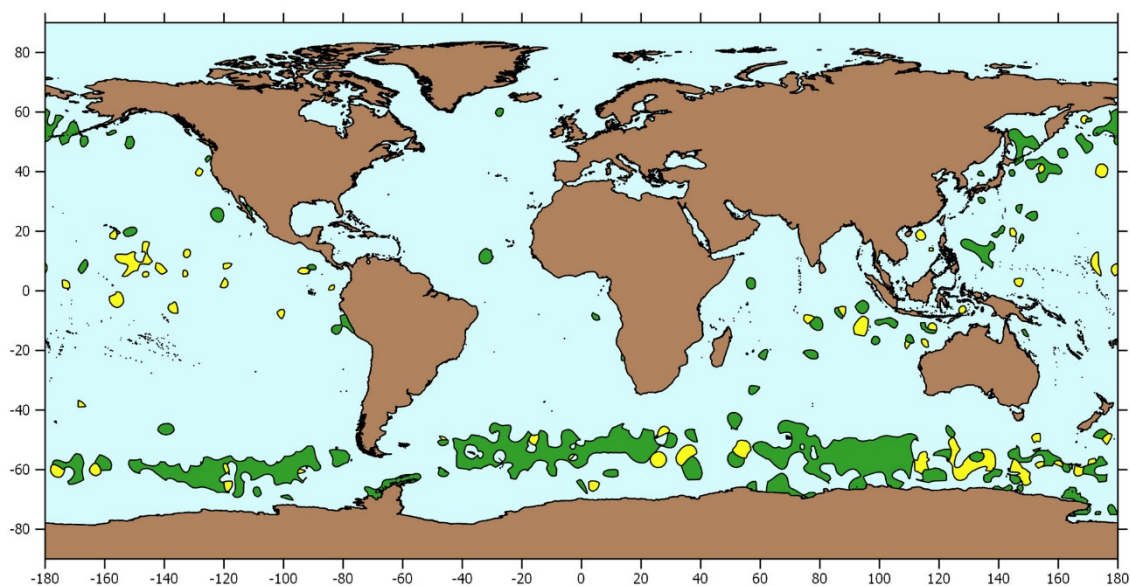
OCEAN COMPARTMENT	Compartment extension (km <sup>2</sup> x 10 <sup>6</sup> )	Radiolarian BSi preservation (mg Si m <sup>-2</sup> y <sup>-1</sup> )			Radiolarian BSi burial flux (Tmol Si y <sup>-1</sup> )		
		Scenario 1 6.8%	Scenario 2 10.7%	Scenario 3 28.7%	Scenario 1 6.8%	Scenario 2 10.7%	Scenario 3 28.7%
radiolarian oozes	5.340	38.74 $\pm$ 8.49	61.17 $\pm$ 13.41	163.91 $\pm$ 35.92	0.01 $\pm$ 0.00	0.01 $\pm$ 0.00	0.03 $\pm$ 0.01
radiolaria-rich diatom oozes	19.464	38.74 $\pm$ 8.49	61.17 $\pm$ 13.41	163.91 $\pm$ 35.92	0.03 $\pm$ 0.01	0.04 $\pm$ 0.01	0.11 $\pm$ 0.02
rest of "radiolarian" ocean	337.076	4.91 $\pm$ 11.98	4.91 $\pm$ 11.98	4.91 $\pm$ 11.98	0.06 $\pm$ 0.10	0.06 $\pm$ 0.10	0.06 $\pm$ 0.10
GLOBAL OCEAN	361.880	--	--	--	0.09 $\pm$ 0.05	0.11 $\pm$ 0.05	0.20 $\pm$ 0.06



**Supplementary Fig. 3 | Buried sponge spicules.** **a-c**, Nearly entire tilostyle buried in 5m of highly carbonated, 4,500 year-old sediments of a *Posidonia oceanica* meadow (core 7). Despite this sediment favoring BSi digestion, both the axial canal (**b**, arrow) and the spicule surface (**c**) show only incipient signs of dissolution, revealed by tiny pits. **d-f**, Spicule fragment (**d**) in the same sediment sample, showing an axial canal (**e**, arrow) that has not yet been widened by dissolution. Likewise, the spicule surface shows only incipient signs of dissolution in the form of small pits (**f**).



**Supplementary Fig. 4 | a**, The burial rate of sponge BSi poorly correlates the rate of sediment deposition, in agreement with a previous study<sup>49</sup>. This is so because sponges are sessile and, unlike in the case of planktonic diatoms, their BSi does not reach the sediment as a silica rain from the water column, but rather through restricted lateral transport and limited resuspension from the decaying bodies. The magnitude of the sponge BSi burial will depend primarily on the local abundance of sponges. The sediment deposition rate will mostly determine the speed at which the sponge BSi gets buried, minimally affecting the magnitude of the sponge BSi burial flux. **b**, Sponge BSi preservation (%) does not correlate total BSi in the sediments. This is apparently shocking, since chemical rules dictate that the level of total BSi in sediments controls the DSi saturation of the interstitial seawater and, therefore, its avidity to dissolve BSi structures, a process well known from diatom frustules. Yet, there is also experimental evidence that sponge BSi is refractory to dissolution in DSi-unsaturated seawater<sup>52</sup> and basic solutions<sup>64</sup>, *this study*, what disrupts the theoretically expected relationship. The reasons for the comparatively high resistance to dissolution of the sponge BSi remain unclear, but its complexation with dissolution-resistant organic molecules such as chitin<sup>65</sup> could be involved.



**Supplementary Fig. 5 | Radiolarian-rich ooze.** Patches of ocean floor where sediments contain abundant skeletons of siliceous radiolarians. Radiolarian oozes are in yellow and radiolarian-rich diatom oozes are in green (modified from Dutkiewicz *et al*<sup>61</sup>; see [Methods](#)).

**Supplementary Methods.** Sediment age was calculated from deposition ratios or age information available in the scientific literature of either the cores themselves or sediments from adjacent sites, as it follows: core 1<sup>31</sup>, core 2<sup>24</sup>, core 3<sup>66</sup>, core 4<sup>23</sup>, core 5<sup>7,8</sup>, core 6<sup>20,21</sup>, core 7<sup>10</sup>, core 8<sup>27,67</sup>, core 9<sup>34,37</sup>, core 10<sup>11</sup>, core 11<sup>35,36</sup>, core 12<sup>40</sup>, core 13<sup>29,30</sup>, core 14<sup>68</sup>, core 15<sup>15</sup>, core 16<sup>42</sup>, core 17<sup>16,17,18</sup>. Sediment biomass was obtained from the wet bulk density, either obtained from the above-cited literature or estimated from core depth through the Tenzer and Gladkikh's regression equation<sup>69</sup>,

$$\rho(D) = [1.66 \pm 0.02] - D \times [(5.1 \pm 0.5) \times 10^{-5}],$$

where " $\rho$ " is density in  $\text{g cm}^{-3}$ , " $D$ " is ocean depth in m, "1.66" is the nominal sediment density of the upper sedimentary layer at sea level, and " $5.1 \times 10^{-5}$ " is a coefficient reflecting that density decreases proportionally (relative to the nominal value) at a rate of  $-0.051 \text{ g cm}^{-3}$ .

Density values of BSi vary across organism types. For sponges, it varies from 2.03 to  $2.13 \text{ g cm}^{-3}$ , depending on the species<sup>70</sup>. Density varies from 1.7 to  $2.1 \text{ g cm}^{-3}$  in radiolarian silica<sup>71</sup>. In the calculations, we have used values of  $2.12 \text{ g cm}^{-3}$  for marine sponges,  $1.9 \text{ g cm}^{-3}$  for radiolarians and  $2.0 \text{ g cm}^{-3}$  for silicoflagellates<sup>72</sup>.

## References

1. Lisitzin AP. *Sedimentation in the world ocean*, vol. 17. Society of Economic Paleontologists and Mineralogists: Tulsa, 1972.
2. Lisitzin AP. Distribution of siliceous microfossils in suspension and in bottom sediments. In: Funnell BM, Riedel WR (eds). *The micropaleontology of oceans*. Cambridge University Press: Cambridge, 1971, pp 173-195.
3. Hurd DC. Interactions of biogenic opal, sediment and seawater in the Central Equatorial Pacific. *Geochim Cosmochim Acta* 1973, **37**(10): 2257-2282.
4. Dittert N, Corrin L, Diepenbroek M, Grobe H, Heinze C, Ragueneau O. Management of (pale-)oceanographic data sets using the PANGAEA information system: the SINOPS example. *Computers & Geosciences* 2002, **28**(7): 789-798.
5. DeMaster DJ. Measuring biogenic silica in marine sediments and suspended matter. In: Hurd DC, Spenser DW (eds). *Marine particles: Analysis and characterization*, vol. Geophysical Monographs 63. American Geophysical Union: Washington, 1991, pp 363-367.
6. Gregoire G, Le Roy P, Ehrhold A, Jouet G, Garlan T. Control factors of Holocene sedimentary infilling in a semi-closed tidal estuarine-like system: the bay of Brest (France). *Mar Geol* 2017, **385**: 84-100.
7. Keigwin LD, Sachs JP, Rosenthal Y. A 1600-year history of the Labrador Current off Nova Scotia. *Climate Dynamics* 2003, **21**(1): 53-62.
8. Piper DJW. Seabed geology of the Canadian eastern continental shelf. *Cont Shelf Res* 1991, **11**(8-10): 1013-1035.
9. Mateo MA, Renom P, Michener RH. Long-term stability in the production of a NW Mediterranean *Posidonia oceanica* (L.) Delile meadow. *Palaeogeography, Palaeoclimatology, Palaeoecology* 2010, **291**: 286-296.
10. Serrano O, Mateo MA, Renom P, Julià R. Characterization of soils beneath a *Posidonia oceanica* meadow. *Geoderma* 2012, **185–186**: 26-36.
11. Nelson CH, Baraza J, Maldonado A, Rodero J, Escutia C, Barber JH. Influence of the Atlantic inflow and Mediterranean outflow currents on Late Quaternary sedimentary facies of the Gulf of Cadiz continental margin. *Mar Geol* 1999, **155**(1-2): 99-129.
12. López-Acosta M, Leynaert A, Grall J, Maldonado M. Silicon consumption kinetics by marine sponges: An assessment of their role at the ecosystem level. *Limnol Oceanogr* 2018, **63**(6): 2508-2522.

13. Beazley L, Wang ZL, Kenchington E, Yashayaev I, Rapp HT, Xavier JR, *et al.* Predicted distribution of the glass sponge *Vazella pourtalesi* on the Scotian Shelf and its persistence in the face of climatic variability. *Plos One* 2018, **13**(10): e0205505.
14. Stevens SH, Moore GF. Deformational and sedimentary processes in trench slope basins of the western Sunda Arc, Indonesia *Mar Geol* 1985, **69**(1-2): 93-112.
15. Dunbar GB, Dickens GR, Carter RM. Sediment flux across the Great Barrier Reef Shelf to the Queensland Trough over the last 300 ky. *Sediment Geol* 2000, **133**(1-2): 49-92.
16. Masqué P, Isla E, Sanchez-Cabeza JA, Palanques A, Bruach JM, Puig P, *et al.* Sediment accumulation rates and carbon fluxes to bottom sediments at the Western Bransfield Strait (Antarctica). *Deep-Sea Res II* 2002, **49**(4-5): 921-933.
17. Isla E, Masqué P, Palanques A, Guillén J, Puig P, Sanchez-Cabeza JA. Sedimentation of biogenic constituents during the last century in western Bransfield and Gerlache Straits, Antarctica: a relation to currents, primary production, and sea floor relief. *Mar Geol* 2004, **209**(1): 265-277.
18. Willmott V, Domack EW, Canals M, Brachfeld S. A high resolution relative paleointensity record from the Gerlache-Boyd paleo-ice stream region, northern Antarctic Peninsula. *Quatern Res* 2006, **66**(1): 1-11.
19. Serrano A, Gonzalez-Irusta JM, Punzon A, Garcia-Alegre A, Lourido A, Rios P, *et al.* Deep-sea benthic habitats modeling and mapping in a NE Atlantic seamount (Galicia Bank). *Deep-Sea Res I* 2017, **126**: 115-127.
20. Alonso B, Ercilla G, Casas D, Estrada F, Farrán M, García M, *et al.* Late Pleistocene and Holocene sedimentary facies on the SW Galicia Bank (Atlantic NW Iberian Peninsula). *Mar Geol* 2008, **249**(1-2): 46-63.
21. Rey D, Rubio B, Mohamed K, Vilas F, Alonso B, Ercilla G, *et al.* Detrital and early diagenetic processes in Late Pleistocene and Holocene sediments from the SW Galicia Bank inferred from high-resolution enviromagnetic and geochemical records. *Mar Geol* 2008, **249**(1-2): 64-92.
22. Murillo FJ, Serrano A, Kenchington E, Mora J. Epibenthic assemblages of the Tail of the Grand Bank and Flemish Cap (northwest Atlantic) in relation to environmental parameters and trawling intensity. *Deep-Sea Res I* 2016, **109**: 99-122.
23. Weitzman J, Ledger S, Stacey CD, Strathdee G, Piper DJW, Jarrett KA, *et al.* Logs of short push cores, deep-water margin of Flemish Cap and the eastern Grand Banks of Newfoundland: Geological Survey of Canada; 2014.

24. Murillo FJ, Kenchington E, Lawson JM, Li G, Piper DJW. Ancient deep-sea sponge grounds on the Flemish Cap and Grand Bank, northwest Atlantic. *Mar Biol* 2016, **163**(3): 1-11.
25. Heinrich H. Origin and consequences of cyclic ice rafting in the Northeast Atlantic Ocean during the past 130,000 years. *Quatern Res* 1988, **29**: 142-152.
26. Ercilla G, Farrán M, Alonso B, Díaz JI. Pleistocene progradational growth pattern of the northern Catalonia continental shelf (northwestern Mediterranean). *Geo-Marine Letters* 1994, **14**: 264-271.
27. Beaudouin C, Dennielou B, Melki T, Guichard F, Kallel N, Berné S, *et al.* The Late-Quaternary climatic signal recorded in a deep-sea turbiditic levee (Rhône Neofan, Gulf of Lions, NW Mediterranean): palynological constraints. *Sediment Geol* 2004, **172**(1-2): 85-97.
28. Auger PA, Diaz F, Ulses C, Estournel C, Neveux J, Joux F, *et al.* Functioning of the planktonic ecosystem on the Gulf of Lions shelf (NW Mediterranean) during spring and its impact on the carbon deposition: a field data and 3-D modelling combined approach. *Biogeosciences* 2011, **8**(11): 3231-3261.
29. Damuth JE. Late Quaternary sedimentation in the western equatorial Atlantic. *Geol Soc Am Bull* 1977, **88**: 695-710.
30. Embley RW, Langseth MG. Sedimentation processes on the continental rise of northeastern South America. *Mar Geol* 1977, **25**(4): 279-297.
31. Kenyon NH, Ivanov MK, Akhmetzhanov AM. Cold water carbonate mounds and sediment transport on the Northeast Atlantic margin: UNESCO; 1998.
32. Bett BJ, Rice AL. The influence of hexactinellid sponge spicules on the patchy distribution of macrobenthos in the Porcupine Seabight (bathyal NE Atlantic). *Ophelia* 1992, **36**: 217-226.
33. Rice AL, Thurston MH, New AL. Dense aggregations of a hexactinellid sponge, *Pheronema carpenteri*, in the Porcupine Seabight (northeast Atlantic Ocean), and possible causes. *Prog Oceanogr* 1990, **24**: 179-196.
34. Frigola J, Moreno A, Cacho I, Canals M, Sierro FJ, Flores JA, *et al.* Evidence of abrupt changes in Western Mediterranean Deep Water circulation during the last 50 kyr: A high-resolution marine record from the Balearic Sea. *Quatern Int* 2008, **181**(1): 88-104.
35. Cacho I, Grimalt JO, Canals M, Sbaiffi L, Shackleton NJ, Schonfeld J, *et al.* Variability of the western Mediterranean Sea surface temperature during the last

- 25,000 years and its connection with the Northern Hemisphere climatic changes. *Paleoceanography* 2001, **16**(1): 40-52.
36. Nebout NC, Turon JL, Zahn R, Capotondi L, Londeix L, Pahnke K. Enhanced aridity and atmospheric high-pressure stability over the western Mediterranean during the North Atlantic cold events of the past 50 k.y. *Geology* 2002, **30**(10): 863-866.
  37. Sierro FJ, Hodell DA, Curtis JH, Flores J-A, Reguera I, Colmenero-Hidalgo E, *et al.* (Table 1) Age determination of sediment core MD99-2343. *Supplement to: Sierro, FJ et al. (2005): Impact of iceberg melting on Mediterranean thermohaline circulation during Heinrich events. Paleoceanography, 20(2), PA2019, <https://doi.org/10.1029/2004PA001051>: PANGAEA; 2005.*
  38. Stambler N. The Mediterranean Sea - Primary Productivity. In: Goffredo S, Dubinsky Z (eds). *The Mediterranean Sea: Its history and present challenges*. Springer: Dordrecht, 2014, pp 113-121.
  39. Würtz M, Rovere M. *Atlas of the Mediterranean seamounts and seamount-like structures*. IUCN: Gland, Switzerland, 2015.
  40. Volz JB, Mogollon JM, Geibert W, Arbizu PM, Koschinsky A, Kasten S. Natural spatial variability of depositional conditions, biogeochemical processes and element fluxes in sediments of the eastern Clarion-Clipperton Check for Zone, Pacific Ocean. *Deep-Sea Research Part I-Oceanographic Research Papers* 2018, **140**: 159-172.
  41. Vanreusel A, Hilario A, Ribeiro PA, Menot L, Arbizu PM. Threatened by mining, polymetallic nodules are required to preserve abyssal epifauna. *Sci Rep* 2016, **6**: 26808.
  42. Jacot Des Combes H, Esper O, De la Rocha CL, Abelmann A, Gersonde R, Yam R, *et al.* Diatom  $\delta^{13}\text{C}$ ,  $\delta^{15}\text{N}$ , and C/N since the Last Glacial Maximum in the Southern Ocean: potential impact of species composition. *Paleoceanography* 2008, **23**(4).
  43. Alvain S, Moulin C, Dandonneau Y, Loisel H. Seasonal distribution and succession of dominant phytoplankton groups in the global ocean: a satellite view. *Global Biogeochem Cycles* 2008, **22**(3): GB3001.
  44. DeMaster DJ. The accumulation and cycling of biogenic silica in the Southern Ocean: revisiting the marine silica budget. *Deep-Sea Res II* 2002, **49**(16): 3155-3167.
  45. Ahlback WJ, McCartney K. Siliceous sponge spicules from site 478: ODP; 1992.
  46. McCartney K. Siliceous sponge spicules from Ocean Drilling Program Leg 114: ODP; 1990.

47. Murray J, Chumley J. The deep-sea deposits of the Atlantic Ocean. *Trans R Soc Edinb* 1924, **54**: 1-252.
48. Rützler K, Macintyre IG. Siliceous sponge spicules in coral reefs sediments. *Mar Biol* 1978, **49**(2): 147-159.
49. Bavestrello G, Cattaneo-Vietti R, Cerrano C, Cerutti S, Sarà M. Contribution of sponge spicules to the composition of biogenic silica in the Ligurian Sea. *Pubbl Staz Zool Napoli Mar Ecol* 1996, **17**(1-3): 41-50.
50. Barthel D, Tendal OS. Sponge spicules in abyssal and bathyal sediments of the NE Atlantic. *Deep-Sea Newsl* 1993, **20**: 15-18.
51. Gutt J, Böhmer A, Dimmler W. Antarctic sponge spicule mats shape macrobenthic diversity and act as a silicon trap. *Mar Ecol Prog Ser* 2013, **480**: 57-71.
52. Maldonado M, Carmona MC, Velásquez Z, Puig A, Cruzado A, López A, *et al.* Siliceous sponges as a silicon sink: An overlooked aspect of the benthopelagic coupling in the marine silicon cycle. *Limnol Oceanogr* 2005, **50**(3): 799-809.
53. Chu JWF, Maldonado M, Yahel G, Leys SP. Glass sponge reefs as a silicon sink. *Mar Ecol Prog Ser* 2011, **441**: 1-14.
54. Maldonado M, Aguilar R, Bannister RJ, Bell JJ, Conway KW, Dayton PK, *et al.* Sponge grounds as key marine habitats: A synthetic review of types, structure, functional roles, and conservation concerns. In: Rossi S, Bramanti L, Gori A, Orejas C (eds). *Marine animal forests: The ecology of benthic biodiversity hotspots*. Springer International Publishing: Cham, 2017, pp 145-183.
55. Dayton PK. Interdecadal variation in an Antarctic sponge and its predator from oceanographic climate shifts. *Science* 1989, **245**: 1484-1486.
56. Maldonado M, Ribes M, Van Duyl FC. Nutrient fluxes through sponges: biology, budgets, and ecological implications. *Adv Mar Biol* 2012, **62**: 114-182.
57. Conway KW, Barrie JV, Austin WC, Luternauer JL. Holocene sponge bioherms on the western Canadian continental shelf. *Cont Shelf Res* 1991, **11**(8-10): 771-790.
58. Jochum KP, Wang X, Vennemann TW, Sinha B, Müller WEG. Siliceous deep-sea sponge *Monorhaphis chuni*: A potential paleoclimate archive in ancient animals. *Chem Geol* 2012, **300-301**: 143-151.
59. Ragueneau O, Chauvaud L, Moriceau B, Leynaert A, Thouzeau G, Donval A, *et al.* Biodeposition by an invasive suspension feeder impacts the biogeochemical cycle of Si in a coastal ecosystem (Bay of Brest, France). *Biogeochemistry* 2005, **75**(1): 19-41.

60. DeMaster DJ. The supply and accumulation of silica in the marine environment. *Geochim Cosmochim Acta* 1981, **45**(10): 1715-1732.
61. Dutkiewicz A, Müller RD, O'Callaghan S, Jónasson H. Census of seafloor sediments in the world's ocean. *Geology* 2016, **43**(9): 795-798.
62. Tréguer PJ. The Southern Ocean silica cycle. *C R Geoscience* 2014, **346**(11): 279-286.
63. Bavestrello G, Bonito M, Sarà M. Silica content and spicular size variation during an annual cycle in *Chondrilla nucula* Schmidt (Porifera, Demospongiae) in the Ligurian Sea. *Scientia Marina* 1993, **57**(4): 421-425.
64. Kamatani A, Oku O. Measuring biogenic silica in marine sediments. *Mar Chem* 2000, **68**(3): 219-229.
65. Ehrlich H, Maldonado M, Parker AR, Kulchin YN, Schilling J, Köhler B, *et al.* Supercontinuum generation in naturally occurring glass sponges spicules. *Adv Opt Mater* 2016, **4**(10): 1608-1613.
66. Gregoire G, Le Roy P, Ehrhold A, Jouet G, Garlan T. Control factors of Holocene sedimentary infilling in a semi-closed tidal estuarine-like system: the bay of Brest (France). *Marine Geology* 2017, **385**(Supplement C): 84-100.
67. Miralles J, Radakovitch O, Aloisi JC. 210Pb sedimentation rates from the Northwestern Mediterranean margin. *Mar Geol* 2005, **216**(3): 155-167.
68. Sumner EJ, Siti MI, McNeill LC, Talling PJ, Henstock TJ, Wynn RB, *et al.* Can turbidites be used to reconstruct a paleoearthquake record for the central Sumatran margin? *Geology* 2013, **41**(7): 763-766.
69. Tenzer R, Gladkikh V. Assessment of density variations of marine sediments with ocean and sediment depths. *Sci World J* 2014, **2014**: 1-9.
70. Sandford F. Physical and chemical analysis of the siliceous skeletons in six sponges of two groups (demospongiae and hexactinellida). *Microscopy Research and Technique* 2003, **62**(4): 336-355.
71. DeMaster DJ. The diagenesis of biogenic silica: Chemical transformations occurring in the water column, seabed, and crust. In: Mackenzie FT (ed). *Treatise on Geochemistry, Volume 7 : Sediments, diagenesis, and sedimentary rocks*, vol. 7. Elsevier, 2003, pp 97-98.
72. Hurd DC. Physical and chemical properties of siliceous skeletons. In: Aston SR (ed). *Silicon geochemistry and biochemistry*. Academic Press: London, 1983, pp 187-244.